8

Magnetic Resonance Imaging of the Thoracic Aorta: A Review of Technical and Clinical Aspects, Including Its Use in the Evaluation of Aneurysms and Acute Vascular Conditions

Vasco Herédia[1,2], Miguel Ramalho[1,3], Sérgio Duarte[4], Rafael O.P. de Campos[1], Mateus Hernandez[1], Nuno Jalles Tavares[5] and Richard C. Semelka[1]

[1]*Department of Radiology, University of North Carolina at Chapel Hill, Chapel Hill,*
[2]*Department of Radiology, Hospital Espírito Santo, Évora,*
[3]*Department of Radiology, Hospital Garcia de Orta, Lisbon,*
[4]*Department of Radiology, Hospital da Luz, Lisbon,*
[5]*Caselas MR Center, Lisbon,*
[1]*USA*
[2,3,4,5]*Portugal*

1. Introduction

Recent advances in non-invasive cross sectional imaging methods, such as CT and MRI have replaced most of invasive angiographic procedures with less cost and morbidity. Magnetic Resonance angiography (MRA) has gained broad acceptance and is fast becoming a routine in evaluation of the thoracic aorta. Latest developments in gradient hardware, pulse sequences, multiarray receiver coils and parallel imaging techniques as well as improved sequence performance of both 1.5T and 3T allows for detailed and comprehensive evaluation of the thoracic aorta and great vessels without exposure to ionizing radiation or iodinated contrast agents. Because MRA does not require the use of ionizing radiation, it can be performed more safely as repeat studies in the follow-up of thoracic aortic disease. Also, contrast-enhanced MRA uses a lesser volume of intravenous contrast agents, and is much less likely to result in contrast-induced in nephropathy compared with CT with iodine contrast, which may be particularly relevant since patients with aortic disease are often old, and frequently suffer from some extent of renal insufficiency. Another benefit that is intrinsic to MRI is the exquisite contrast resolution and the ability to perform a variety of techniques based on different physical principles. For example, for patients at risk of nephrogenic systemic fibrosis (NSF), non-contrast-enhanced MRA techniques may be considered, generally with good morphologic assessment. Not every MRA technique yields equivalent results in similar situations, and therefore, it is important to understand the

advantages and limitations of each technique. Furthermore, based on the intrinsic sensitivity to flow and motion, MRI offers the possibility of acquiring functional information that is of incremental value to the morphological MRA study.
The utility of MRA has been further improved by the addition of new intravenous contrast agents and the proliferation of post processing techniques, many of which are largely automated on commercially available workstations.
In this chapter we will discuss the current role of MRI in the assessment of the thoracic aorta; the available imaging techniques, and illustrate the application of these techniques to the diagnosis of acute thoracic syndrome related to the aorta.

2. MRA techniques

Magnetic resonance imaging (MRI) can use several different techniques for the evaluation of the aorta, each with advantages and disadvantages. Therefore examinations often require different and complementary approaches, according to the patient and clinical condition.
Magnetic resonance imaging of the aorta and pulmonary arteries is mainly dependent on a morphological evaluation, either alone or combined with a functional evaluation. The goals of the morphological evaluation are to provide information on the vessel location, diameter, wall characteristics, lumen patency and anatomical relations, including adjacent tissues and vessel branches. Unlike CT, MR can additionally provide vascular functional assessment, which can be useful in selected clinical settings. Many advanced practices are converging toward a subset of techniques that are fast, reliable, and reproducible. In the subheadings below, the authors will describe in more detail the different imaging approaches that can be used in the study of the thoracic aorta.

2.1 Gadolinium-enhanced MR angiography techniques

The use of gadolinium-based contrast agents (GBCA) has dramatically expanded the clinical utility of MRA. Gadolinium-enhanced MR angiography techniques can be highly spatially resolved, usually called contrast enhanced-MRA (CE-MRA), or highly temporally resolved, also called Time-resolved MRA (TR-MRA).
Many of the important advances in vascular MR imaging have involved evolution of CE-MRA, resulting in high-quality images in a single breath-hold (Sodickson, 2000; Lohan 2008). The most commonly used approach for CE-MRA is a 3D gradient echo (3D-GRE), allowing thin contiguous image partitions to be obtained during a single breath-hold. CE-MRA using a heavily T1-weighted 3D-GRE technique has become the mainstay of MR study of the vascular abnormalities of the thoracic aorta (Prince, 1993, 1996; Krinsky 1996, 1997; Sakamoto, 2010) (Fig1).
After the intravenous injection of a bolus of a GBCA, there is a T1-shortening of blood so that the blood appears bright irrespective of flow patterns or velocities. Usually, a standard dose (0.1 mL/kg bodyweight) of a GBCA is administered at a flow rate of 2-5 mL per second, followed by a saline flush of 20 mL injected at the same flow rate immediately after contrast administration, to achieve a compact bolus. Because signal enhancement and overall image quality of CE-MRA depends on the intra-arterial concentration of the GBCA, the correct timing of imaging after contrast material injection is fundamental (Sakamoto, 2010). Nevertheless, gadolinium has a larger window of visibility than iodine on CT images, which renders timing of data acquisition less critical than on CT.

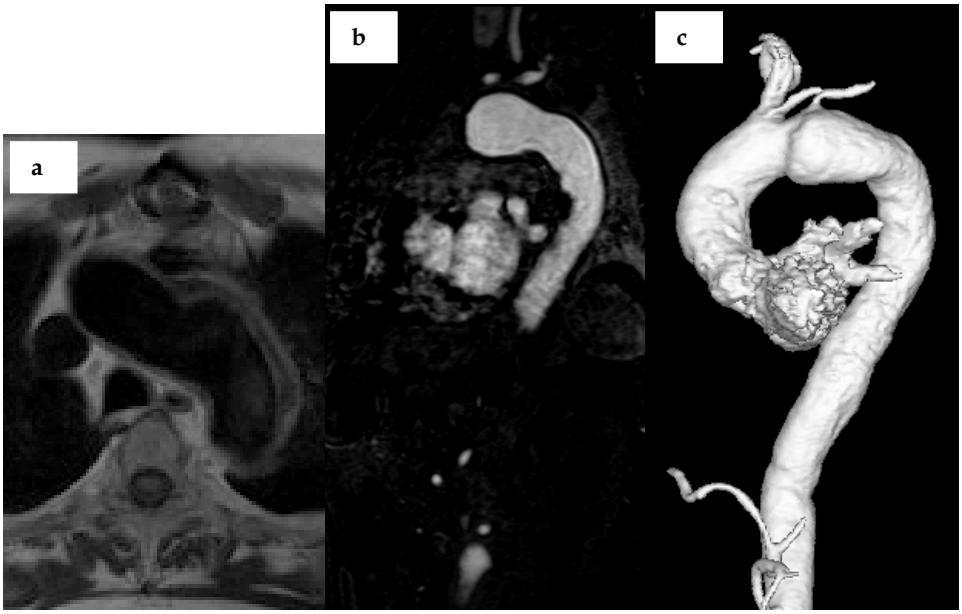

Fig. 1. A 6cm x 4cm saccular aneurysm at the aortic arch is depicted using the black blood technique (a). Black-blood imaging allows visualization of the involved aortic wall, facilitating accurate luminal and wall-to-wall diameter measurement. Source image of 3D parasagital CE-MRA acquisition (b) did not allow confident depiction of the aneurysm. Note the reduced signal from background (stationary) tissue, as there is insufficient time for recovery of longitudinal magnetization. Post processing MRA techniques like volume rendering (c) with multiple projections allowed a confidant diagnosis of this process.

Several methods are used to determine the optimal delay between the start of intravenous contrast material injection and the start of image acquisition, including injection of a test bolus using a small amount of contrast material, automatic triggering, and MR fluoroscopy (Sakamoto, 2010; Hany, 1997; Foo, 1997; Riederer, 2000). More recently, all major MRI system vendors have introduced real-time bolus monitoring software packages and these are now considered the state-of-the art for CE-MRA. Real-time bolus monitoring allows the operator to inject the total volume of contrast material, and to proceed with the 3D CE-MRA acquisition when the desired signal enhancement in the arterial bed of interest has been detected by the MR system, or by visual feedback by the operating technologist. Real-time MR fluoroscopic technique also integrates a monitoring phase and an imaging phase into a single pulse sequence. With the MR fluoroscopic method, monitoring is performed by using a continuous fast two-dimensional (2D) gradient-echo pulse sequence with imaging centered over the vascular bed.

The dose of contrast necessary to perform thoracic aorta CE-MRA varies by scanner, type of gadolinium-based contrast agent and operator experience. Thoracic aorta CE-MRA can be adequately performed with approximately 20mL or less of GBCA. MultiHance® (gadobenate dimeglumine) has greater T1 shortening than the purely extracellular GBCAs currently available, leading some centers like ours, to use this agent at a lower dose (half-dose or 0.5mmol/KG) than would be used with typical extracellular agents. An additional attractive feature of Multihance is mild protein-binding that increases intravascular dwell time.

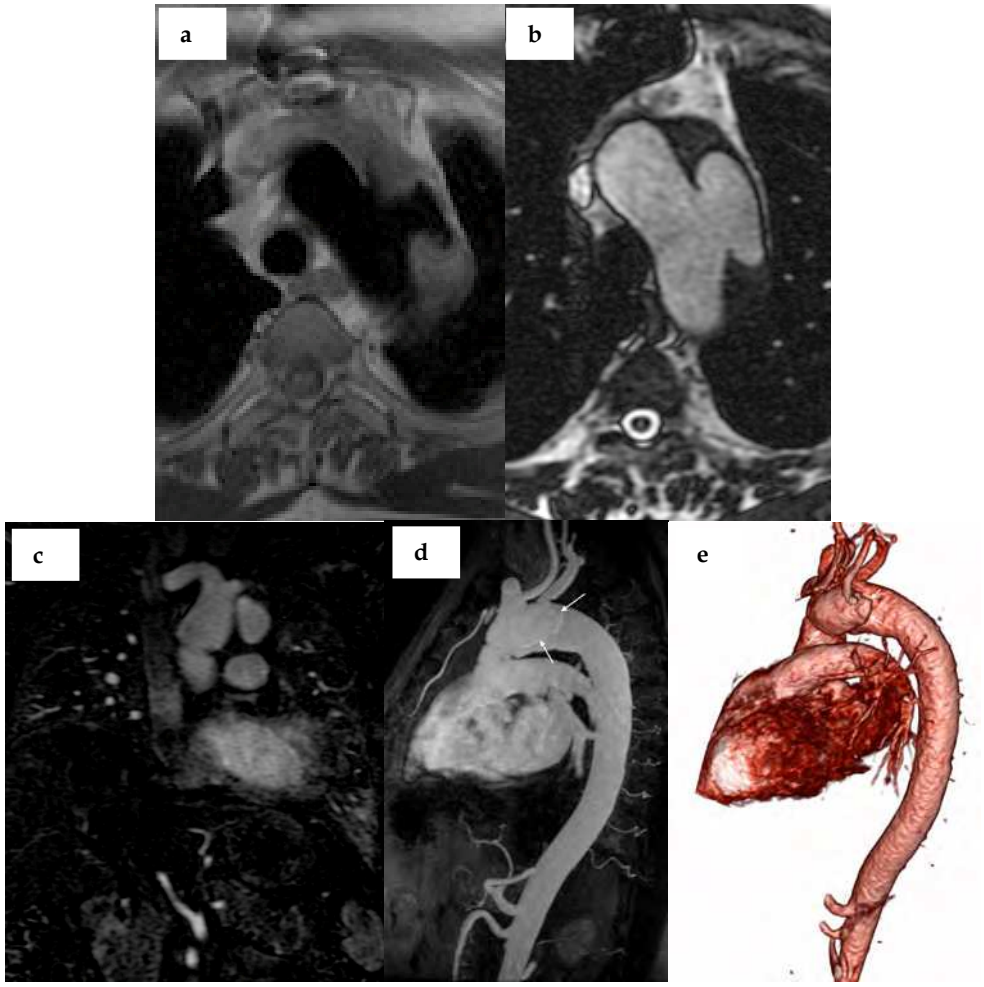

Fig. 2. Aortic pseudoaneurysm in a 48 year-old man, a complication of a previous repair of an aortic aneurysm. Axial black-blood spin-echo (a) and single-shot SSFP (b) images showed a left pseudoaneurysm at the level of the aortic arch. Coronal MPR showed direct communication with the true aortic lumen (c). MIP and volume-rendered full-thickness from CE-MRA examination (d, e) displays the morphology and location of the pseudoaneurysm.

2.1.1 Steady-state contrast enhanced MRA and blood pool contrast agents

Besides dynamic imaging of the arterial-dominant phase after single bolus injection of an extracellular GBCA (first-pass MRA), extended imaging during the steady state of the contrast agent can be performed: this is called steady-state contrast enhanced MRA (Klessen, 2007; Hartmann, 2006; Nissen, 2009). With this technique, specific contrast agents may be

used, blood-pool agents, allowing imaging acquisition up to one hour after contrast administration (Hartmann, 2006).

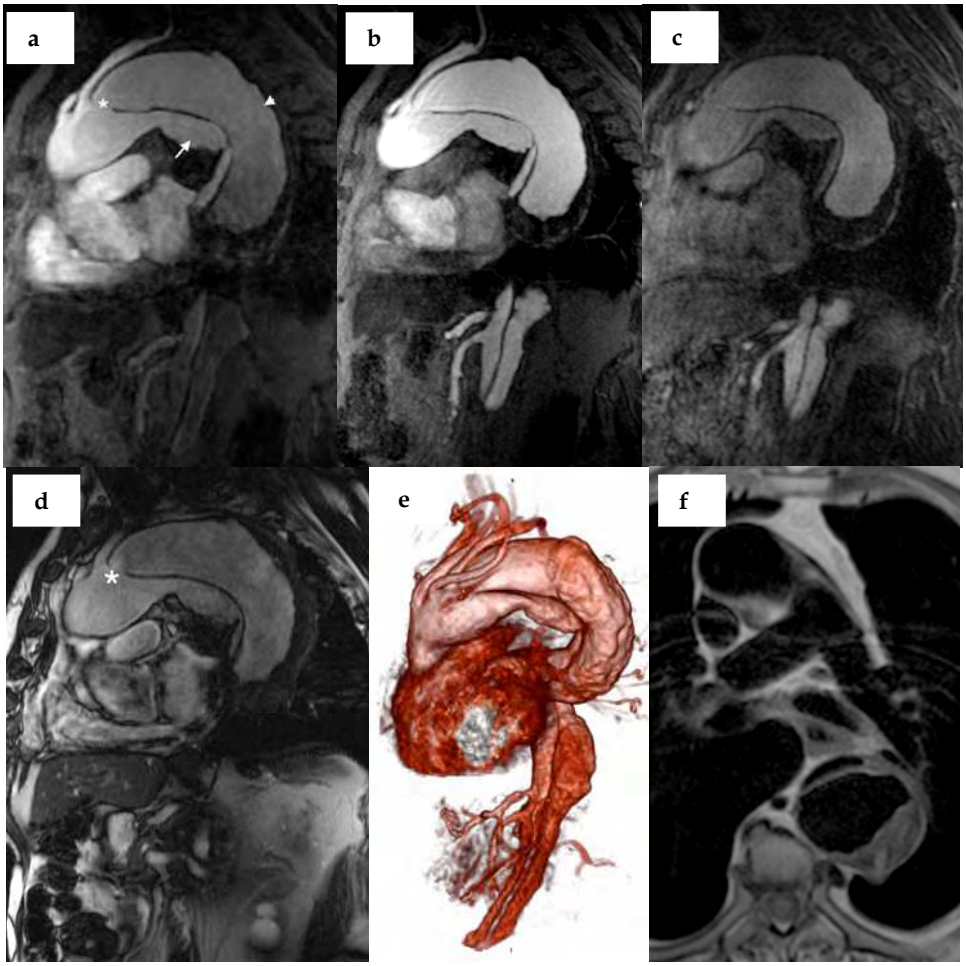

Fig. 3. Oblique sagittal images from a time-resolved MRA of the chest in a 83 year-old male with a Stanford type B aortic dissection. Using a TR-MRA technique it is possible to demonstrate delayed filling of the false lumen (a). There is a dissection flap originating in the aortic arch distal to the origin of the left subclavian artery. Arch vessels that arise from the true lumen and are not involved by dissection. Delayed phases show the distal extent of the false lumen (b, c), with late higher overall enhancement compared to the true lumen (c). The anatomic details of the dissected aorta are somewhat difficult to recognize on volume rendered images (e). Parasagittal reformatted TR-MRA and bSSFP (asterisk, a, d) images clearly depict the intimal flap and also the entry site. Black-blood images (f) show a compressed true lumen due to a dilated false lumen.

Blood pool contrast agents have a prolonged intravascular phase, which means that a wide window of opportunity exists for imaging the blood vessels after contrast agent administration. Gadofosveset trisodium (Ablavar®, Vasovist®) is the first blood pool contrast agent FDA approved for routine clinical use. Gadofosveset is characterized by a lipophilic side chain, which leads to a transient, reversible and non-covalent binding to serum albumin (Lauffer, 1998). The transient protein interaction increases T1-relaxtivity four to five times compared to standard extracellular gadolinium chelates at 1.5 T (Nissen, 2009; Rohrer, 2005; Caravan, 2007), resulting in prolonged blood pool enhancement, which is particularly beneficial for vascular imaging. This can be utilized for higher spatial resolution scanning and greater anatomic coverage. Maximum signal enhancement using this contrast agent on MRA is independent of the injection rate used (Nissen, 2009). Nevertheless, first-pass arterial phase imaging should be performed when possible to avoid interference from venous structures, with steady-state CE-MRA used as a complementary acquisition. Gadofosveset can be used for these two types of CE-MRA with a single dose. It remains longer in the intravascular compartment, allowing several repetitions of the CE-MRA sequences after the initiation of contrast injection. It is possible then to choose the acquisition (both in time and imaging plane) that best displays the vessels of interest for image interpretation.

2.1.2 MRA Post-processing and imaging planes

Interpretation of MR images usually is done with the aid of a computer workstation on which individual source images are analyzed and postprocessing techniques, such as maximum intensity projection (MIP) reformation, volume rendering and multiplanar reformation of the images are performed (Fig 2). MIP images can be obtained quickly, and permit a 3D appreciation of anatomy, which can be useful both for the radiologist and for the clinician, as these resemble catheter angiograms, and are therefore the most widely used post-processing technique. MIP reconstruction involves display of the highest signal intensity voxels within each projection ray to create pixels on the final image. These images must be viewed in multiple projections to detect findings that might be otherwise obscured by overlapping structures with higher signal intensity. Volume rendering uses the entire volume of data for image reconstruction. Volume rendering assigns groups of voxels an opacity score from 0% (transparent) to 100% (completely opaque).

Multiplanar (MPR) and curved reformations allow rapid assessment of MRA data in any plane avoiding problems with vessel overlap and background projection. MPR compresses the full volume of data in a single plane.

Comprehensive thoracic aortic evaluation necessitates that images are acquired in several complementary planes, such that the entire course is fully evaluated. Direct coronal and sagittal images may address shortcomings of true axial views, a parasagittal oblique plane to the ascending, transverse, and descending aorta, is recommended such that subtle abnormalities of the arch may be confidently excluded. This imaging plane also is beneficial in aortic dissection, demonstrating the extent of intimal dissection flaps and their relationship to the origins of the supra-aortic branch vessels. In the presence of aortic dissection or aneurysmal dilatation, particularly when involving the ascending portion of the thoracic aorta, cine imaging of the left ventricular outflow tract represents an essential component to the evaluation of the effect of such pathology on ventricular function.

Fig. 4. Ascending aortic aneurysm. Axial black-blood imaging of the aorta through the upper mediastinum at the level of the right pulmonary artery (a). There is homogeneous suppression of luminal blood signal, increasing the conspicuity of the vessel wall.

2.1.3 Time-resolved MR angiography (TR-MRA)

If dynamic information related to direction or rate of vascular enhancement is considered necessary, Time-resolved MR angiography (TR-MRA) techniques can provide this temporal resolution during the vascular phases of enhancement, with a compromise regarding spatial resolution. These techniques are widely available on modern equipments and have become routinely used in many medical centers; TR-MRA can have a complementary or alternative role to conventional CE-MRA and has been advocated by some authors when a comprehensive evaluation of the thoracic vasculature is warranted (Lohan, 2008b).

Dedicated time-resolved MRA sequences such as TRICKS (time-resolved imaging of contrast kinetics), TWIST (time-resolved angiography with stochastic trajectories), or 4D Track (4D time-resolved MRA with Keyhole), can be used to collect data continuously after GBCA injection during a single breath-hold. TR-MRA represents a powerful complement to conventional 3-D CE-MRA. A complementary TR-MRA allows dynamic evaluation of circulatory patency, confidant separation of the arterial and venous phases of luminal enhancement (Lohan, 2008). Patients who have severe respiratory disease and very limited breath-hold capabilities can be examined (Lohan, 2008; Griffin, 2009). Time-resolved CE-MRA is independent of the bolus timing, because the contrast injection and the MR imaging sequence are started simultaneously. TR-MRA may be of particular value in the evaluation of inhomogeneous aortic flow and dissections, showing the opacification of true and false lumens on multiple phases of enhancement (Fig3) (Lohan, 2008; Schoenberg, 1999).

2.1.4 Patient preparation for contrast-enhanced MRA

Patient preparation used has been described elsewhere (Schneider, 2005): In addition to screening for the usual contraindications for MR scanning (e.g. pacemakers) and for the use of GBCA (e.g. pregnancy), patients scheduled for a CE-MRA examination should also be asked about underlying pulmonary disease and their ability to hold their breath. If

necessary, proper coaching is performed in advance and breath holding is optimized by the use of supplemental oxygen and hyperventilation (Marks, 1997). Patients should also be asked about prior interventions, especially vascular or endovascular procedures. Knowledge of extra-anatomic bypass grafts or stent grafts will ensure proper scan prescription and planning.

Patients are checked for venous access. Ideally, for CE-MRA, the intravenous catheter is placed in the antecubital fossa and should be sufficiently large (i.e. at least 22 gauge) to support a bolus rate of at least 2 mL/sec. When imaging the aortic arch and great vessel origins, it is preferable to place the intravenous catheter in the right arm, as left sided venous contrast administration can cause T2* artifacts due to the high concentration of the GBCA within the left brachiocephalic vein en route to the right heart. This can be mistaken for a proximal great vessel stenosis (Lee, 2000).

2.2 Gadolinium-based contrast agents and nephrogenic systemic fibrosis (NSF)

MRA using a GBCA has become the mainstay of high-quality MR imaging of the thoracic vasculature. This reflects its high spatial and temporal resolution, and avoidance of ionizing radiation and of nephrotoxicity related to iodine-based contrast agents, which are utilized in CT. There are however, specific safety conditions that are related to the use of GBCA, such as high-risk patients for nephrogenic systemic fibrosis (NSF), or pregnant patients. Limited intravenous access also may obviate contrast use. Considering NSF and gadolinium, it has been shown that not all agents have the same risk for NSF, and that volume of contrast and cumulative dose influenced the presence and severity of NSF. The use of stable GBCAs are recommended such as macrocyclic agents (eg: Prohance, Gadovist, Dotarem) or ionic Linear with partial hepatobiliary elimination and high T1 relaxation (Gadofosveset or Gadobenate dimeglumine) at risk patients (Wertman, 2008; Altun, 2009a, 2009b; Martin, 2009). Reducing the dose, while maintaining diagnostic information, is also important (Altun, 2009b). Half-dose (0,5mmol/Kg) Gadobenate dimeglumine has been shown to provide diagnostic quality examinations in abdominal studies, including vascular imaging. It is the authors' experience that the same diagnostic results can be achieved in thoracic imaging, when higher doses are not recommended for safety concerns.

Recently, the use of quarter-dose (0,025mmol/Kg) Gadobenate dimeglumine at 3T has been associated with diagnostic images in the abdomen (De Campos, 2011). It is likely that this can also be achieved in thoracic vascular imaging, providing vascular diagnostic imaging of the thorax, either alone or in combination with other techniques, such as TR-MRA and/or noncontrast-enhanced MRA, in selected cases. It should be noted that the relative risk for developing contrast induced nephropathy with iodinated contrast agents in patients with chronic renal failure generally far exceeds the risk of NSF. There is no measurable risk of NSF occurring in patients with mild to moderate (stage 3) chronic renal failure using GBCAs, whereas these patients are at risk for contrast induced nephropathy (Altun, 2009b, Martin 2009).

2.3 Noncontrast-enhanced MR angiography

Over the last decade, contrast-enhanced MR angiography (CE-MRA) techniques (Prince, 1996; Krinsky, 1999; Korosec, 1996) have largely replaced unenhanced MRA techniques for the evaluation of the thoracic aorta because of their high spatial resolution and reliability. In recent years, with the concern about NSF, along with concerns about ionizing radiation and nephrotoxicity of iodinated contrast agents, non-contrast MRA, have re-emerged as important techniques, especially bright blood steady state free precession techniques.

2.3.1 "Bright blood" MR angiography

Non-contrast enhanced "bright blood" vascular imaging includes Steady-state free-precession (SSFP), Time-of-flight (TOF) and Phase-contrast (PC) MR angiography.

Steady-state free-precession (SSFP) sequence (TrueFISP, balanced FFE, FIESTA) is a bright blood technique, with short TE and TR sequences, that has become widely available (Sakamoto, 2010;Earls, 2002; Pereles, 2002). With SSFP, intraluminal signal generally is very high and homogenous even in cases of turbulent flow because this sequence depends mainly on a function of the T2/T1 ratio (Sakamoto, 2010).

SSFP images can be acquired in both breath-hold and free-breathing manners, either with or without ECG-gate and Navigator/ respiratory triggered (Bi, 2005; Amano, 2008). SSFP can provide rapid bright-blood images with high-contrast resolution, free-breathing real-time steady-state free precession techniques allow for a fast non-ECG gated, non–contrast enhanced MRA that may be useful in critically ill patients (Pereles, 2002; Gebker, 2007; Kluge, 2004). A rapid morphologic assessment can be achieved in urgent situations, such as demonstrating aortic abnormalities in unstable patients, for example intimal flaps and false lumens in aortic dissection (Pereles, 2002; Gebker, 2007). Free-breathing cardiac and respiratory-gated 3D SSFP MRA has also been shown valuable in the evaluation of thoracic vessels (Fuchs, 2003; Tomasian, 2008; Krishnam, 2008, 2010), and represents an alternative for free-breathing SSFP MRA.

SSFP sequences can also be acquired in a cine mode, and have become the foundation for cine imaging. Advantages are the higher SNR, shorter imaging duration, and freedom from the reliance on inflow effects for signal generation (Carr, 2001; Lohan, 2008). This sequence has benefited from the application of parallel imaging techniques, allowing high temporal resolution, large FOV imaging of the thoracic aorta, and left ventricular outflow during acceptable breath-holds as low as 5 to 6 seconds. The inherently high blood signal achieved using SSFP throughout a cine acquisition period has been shown to aid evaluation of aortic mural and valvular characteristics and allowing exclusion of the presence of aortic dissection, (Pereles, 2002; Kunz, 2004). SSFP is the most promising of the "bright-blood" non-contrast enhanced MR angiography techniques (Fig2 and 3).

Other techniques, such as time-of-flight (TOF) and phase-contrast (PC) are seldom use for non–contrast-enhanced MR angiography of the thorax because of sensitivity to respiratory and cardiac motions, in-plane saturation, and the need for wide coverage (Prince, 1993;Amano, 2008; McCauley, 1994). These sequences are also time- consuming and susceptible to artifacts. Possible applications exist when vascular flow quantification is warranted.

PC-MRA is an inherently quantitative technique, unlike TOF or CE MRA., allowing for the calculation of flow velocity. With PC-MRA, the signal intensity of blood is proportional to its flow velocity and the direction of flow can be determined on the basis of the direction of the phase shift (Schneider, 2005).

2.3.2 "Black-blood" MR

These techniques are termed black-blood because signal void is created in flowing blood. They consist of either conventional or echo-train spin-echo techniques, usually with ECG-gating, exploiting the contrast between rapidly flowing blood and the aortic wall (Sakamoto, 2010; Czum, 2005; Fattori, 1999; Russo, 2006; Bradley, 1985). Black-blood MRA may be useful for the depiction of intraluminal abnormalities such as dissection flaps and tumor

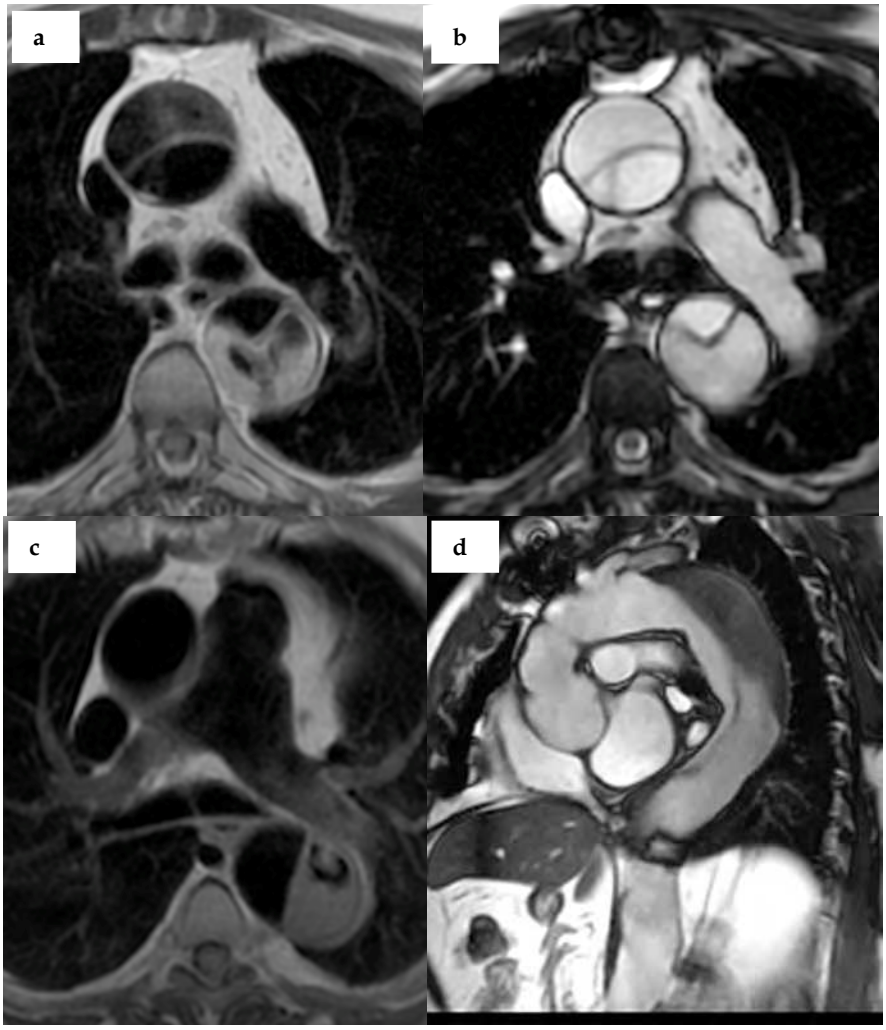

Fig. 5. Two patients with type A dissection. Slow/ turbulent flow may produce high signal in the aortic lumen, artificially simulating wall disease. A simple method of reducing errors is to compare with other sequences. In the first case (a) there is moderate high signal intensity in the false lumen, which correlates with high signal intensity on the bSSFP images (b), associated with slow flow. On the other example (c), the higher signal intensity saw on the spin-echo sequence (black-blood image) correlates with a partial thrombus in the false lumen as low signal intensity on the bSSFP images (d). A simple method of reducing intravascular signal on a black-blood technique is to increase the TE, allowing more time for intravoxel dephasing and for moving excited protons to exit the slice before the refocusing pulse.

thrombus. When vessel wall analysis is desirable, as in aortic conditions such as mural hematoma, black-blood techniques may at times provide a better wall depiction than CE-MRA (Potthast, 2010; Litmanovich, 2009). The goal of black-blood techniques is to eliminate

as much signal as possible from flowing blood in the vessels lumen (Fig4). Luminal signal void occurs because intravascular protons only produce signal if they are exposed to both a 90-degree excitation pulse and subsequent refocusing pulse while travelling through the image slice. Therefore, low flow and entry/exit slice phenomena may produce high signal in the aortic lumen (Fig5), artificially simulating wall disease (Sakamoto, 2010). Echo-train spin-echo techniques are favoured, because of rapid data acquisition (usually in a single breath hold) and improved image resolution (Matsunaga, 2003). T2-weighted single-shot echo-train spin-echo sequences can be obtained as a black blood technique, which may be useful in patients who cannot comply with the necessary breath-holds for alternative imaging (Stehling, 1996; Winterer, 1999).
Usually, black-blood techniques are used in combination with other imaging sequences, most often CE-MRA and/or non-contrast enhanced "bright-blood techniques".

3. Comprehensive thoracic evaluation on vascular MR studies

Although the above-described techniques, especially CE-MRA, can achieve high-quality diagnostic imaging of the thoracic vessels, evaluation of comprehensive chest structures may be necessary. If clinically necessary, the complementary use of T2 weighted single-shot echo-train spin echo and pre-contrast 3D-GRE sequences in axial and coronal planes will provide such information with minimally added time (Fig 6). A basic MRA protocol can be supplemented with additional sequences, based on the suspected clinical condition or pathologic process. Post contrast 3D-GRE MRI visualizes not only the aorta, but also the lungs and other organs and structures in the chest (Bader, 2002; Karabulut, 2002; Altun, 2010) and is usually acquired after the MRA. Blood-pool contrast agents can be beneficial in this setting, allowing for persistently high signal in vessels on delayed acquisition.

4. Clinical conditions

An increasing number of clinical indications for gadolinium-enhanced MRA/MRI have been described, including congenital syndromes, functional imaging of flow and direction, and acquired disease of the aorta. A detailed description of all these indications is beyond the scope of this chapter, and can be found elsewhere (Schneider, 2005). In this review, the authors will focus on some common indications for MRA/MRI imaging of the aorta, aortic aneurysms, and acute aortic syndrome will be discussed. Usually, in these settings, CT is more commonly used than MR, due to its high spatial resolution rapid acquisition, resistance to patient motion, adequate diagnostic capability, and availability of the technique (Bhargavan, 2010; Jha, 2010). Nevertheless, in selected cases, MR may be preferred, such as in young patients, pregnant patients, renal failure, allergy to iodine contrast, or lack of adequate intravenous access. Another setting in which MR is recommended, is in studying patients that will undergo sequential follow up examinations, as a follow-up to initial CT or MR studies, as in the follow-up of aneurysms. In specific conditions, MR can be superior to CT, for example when differentiating false from true lumen in an aortic dissection, using cine-imaging if needed, or when differentiating acute aortic hematoma from atherosclerotic plaque and chronic thrombus (Yucel, 1990).
A combination of morphological assessment techniques and vascular patency techniques is sufficient for most acute conditions. In selected cases, dynamic imaging, usually using TR-

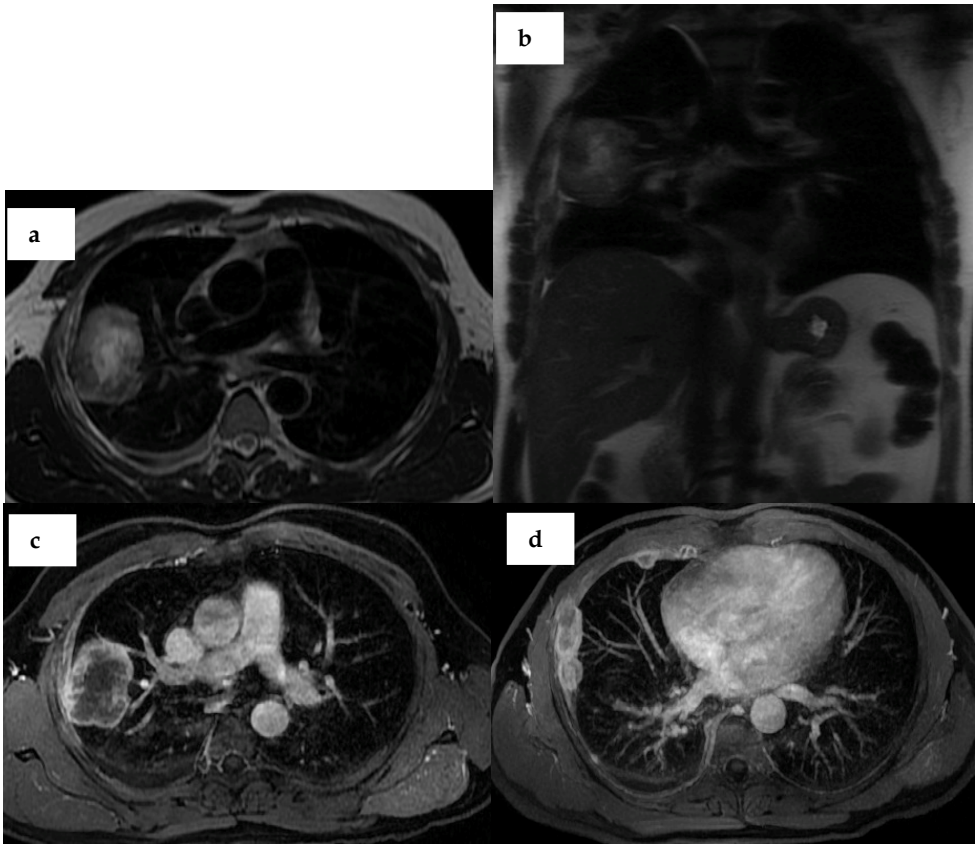

Fig. 6. A 62 year-old male with small cell lung cancer with pleural involvement. Axial double IR black-blood spin-echo MR (a) and coronal T2-weighted single-shot fast spin-echo (b) images clearly showed a pulmonary mass in the right upper lobe. Post contrast T1-weighted 3D-GRE images (c, d) defined the lesion's vascular characteristics and as well as pleural involvement.

MRI or Cine-SSFP can be added to the study, as described below. Using comprehensive imaging protocols provides information, not only on the disease process in question, but other diseases as well. For example, a comprehensive protocol evaluating suspected acute pulmonary embolism can also detect aortic dissection.

4.1 Aortic aneurysm

The normal dimensions of the aorta have been defined based on normative measurements performed in large patient populations (Litmanovich, 2009). An ascending aortic diameter equal to or greater than 4 cm (in individuals younger than 60 years old) and a descending aortic diameter larger than 3 cm is usually considered to indicate dilatation and a diameter equalling or exceeding 1.5 times the expected normal diameter is considered an aneurysm (Litmanovich, 2009). The prevalence of thoracic aortic aneurysms increases with age, with an overall incidence approximating 450 per 100,000 and a 3:1 male predominance

(Bickerstaff, 1982; Litmanovich, 2009). In up to one third of cases, the abdominal aorta is also involved (Bickerstaff, 1982; Litmanovich, 2009) (Fig7). Most thoracic aneurysms are

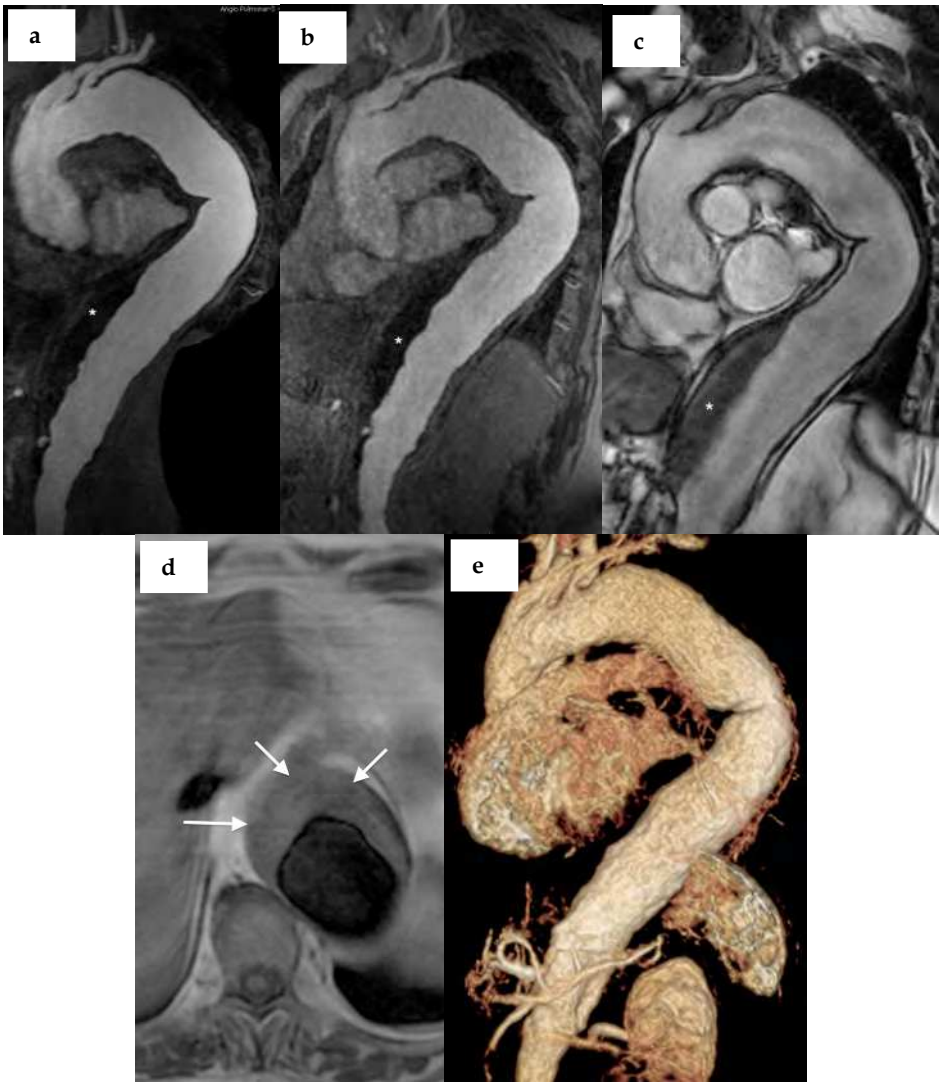

Fig. 7. A 77-year-old male with diffuse long-standing atherosclerotic thoraco-abdominal aneurysm. MIP CE-MRA (a) and TR-MRA (b) images clearly depict the diffuse thoracic aorta dilatation with mural thrombus in the descending aorta (asterisk, A, B) and irregular contour due to severe atherosclerosis. These features are also well appreciated in the bSSFP images (c). Characterization of the aortic wall and thrombus is better preformed with a black-blood sequence (d) like a double inversion spin-echo techniques. With volume rendering (e) the entire volume of data is used in data reconstruction.

atherosclerotic (Tatli, 2004; Litmanovich, 2009). Infection, inflammation, syphilis, and cystic medial necrosis are other causes for aortic aneurysms, the last being the most common cause of an aneurysm isolated to the ascending aorta. Cystic medial necrosis is usually associated with Marfan syndrome but can also be idiopathic (Litmanovich, 2009). In Marfan syndrome, the classic imaging features include a pear-shaped aneurysmal ascending aorta with smooth tapering to a normal aortic arch (Litmanovich, 2009) (Fig 8). Thoracic aortic aneurysms can also be divided into true and false (or pseudoaneurysms), according to their pathologic

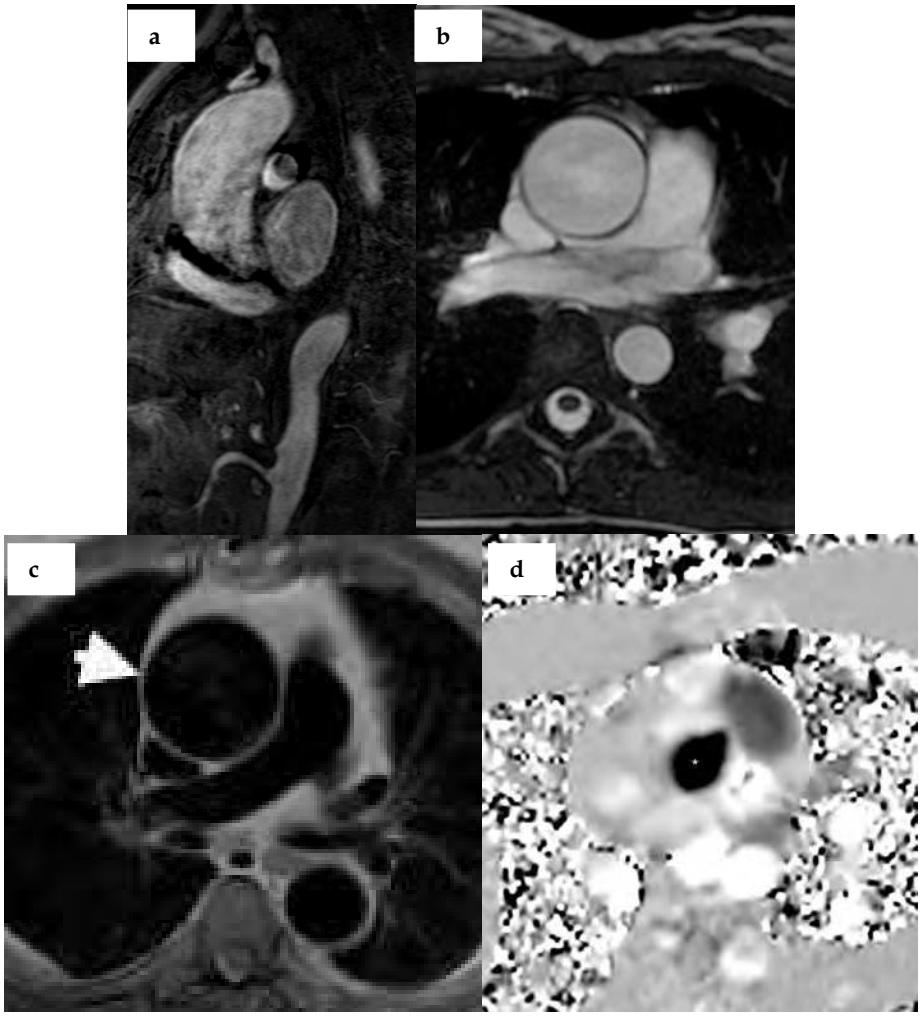

Fig. 8. Fusiform ascending aortic aneurysm in a patient with Marfan syndrome, depicted on CE-MRA (a), bSSFP (b) and on black blood (c) images. Phase contrast flow quantification at the level of the aortic valve (d) shows the characteristic fish-mouth appearance of bicuspid aortic valve, a common addition of aortic aneurysm.

features. In true aneurysms, all layers of the aortic wall are involved. A pseudoaneurysm represents enlargement of the artery resulting from blood accumulating beyond the intimal layer and typically trapped within the serosa or outer layer of the arterial wall (Fig2). Aetiology may be related to ruptured atheroma, dissection, or trauma. When resulting from trauma, the aortic isthmus is more frequently affected by pseudoaneurysms, whereas penetrating aortic ulcer usually occurs in the descending aorta (Litmanovich, 2009; Boiselle, 2007).

True aortic aneurysms are usually fusiform in shape, involving the entire circumference of the aorta, and often extend over a significant length of the vessel, although saccular aneurysms can occasionally be found (Fig1). Pseudoaneurysms are usually saccular, with a narrow neck at the origin in the aorta. The presence of a wide neck in a saccular aneurysm suggests a mycotic origin. These aneurysms have a tendency to involve the ascending aorta, likely because of its proximity to the heart and suspected extension from endocarditis (Boiselle, 2007).

It is important to evaluate eventual extension of thoracic aortic aneurysms to the abdominal aorta, as there are therapeutic implications (Yu, 2007). Thoraco-abdominal aneurysms include Type I (involving the descending thoracic aorta below the origin of the left subclavian artery and the upper abdominal aorta); Type II (involving both the thoracic descending aorta and most of the abdominal aorta); Type III (lower portion of the thoracic aorta) and Type IV (begins at the diaphragm and extends caudally) (Crawford, 1986; Litmanovich, 2009).

When imaging an aortic aneurysm, it is important to exactly evaluate the maximal diameter, the length of the aneurysm, and involvement of major branch vessels (Bonser, 2000). Also, the most frequent complications of aortic aneurysm - mass effect, dissection, and rupture - are related to size. The mean rate of dilatation for thoracic aortic aneurysm is 0.12 cm per year (Coady, 1997). The risk of rupture increases with increasing aortic diameter, with a high risk of complications (rupture and dissection) at 6 cm for the ascending and 7 cm for the descending thoracic aorta (Elefteriades, 2002, 2005). CE-MRA/MRI is generally suitable for this evaluation. It allows the study of the extent of an aneurysm and its relationship to the aortic branches, with reproducible results (Prince, 1996; Krinsky, 1997; Debatin, 1998; Neimatallah, 1999). Breath-hold non ECG-gated CE-MRA is nevertheless more prone to motion artifacts and blurring at the aortic root, with potential implications for treatment planning (Potthast, 2010; Cigarroa, 1993). Non-contrast enhanced ECG-gated 3D-SSFP has shown good results in aneurysm imaging, providing good assessment of diameter, lumen patency and topographic evaluation, including the aortic root (Krishnam, 2008; Potthast, 2010). It can also be used as a cine technique allowing for evaluation of the aortic valve in patients with ascending aortic aneurysms, providing crucial information for treatment planning (Sakamoto, 2010).

Use of the sagittal or oblique sagittal plane allows accurate assessment of the location and extent of the aneurysm and avoids partial volume effects. With CE-MRA, aneurysm measurements should be obtained from source images where the vessel wall is visible, because MIP images represent a cast of the lumen alone, and therefore, underestimates aneurysm dimensions (Sakamoto, 2010). Standard spin echo images and precontrast 3D-GRE also are helpful in evaluating changes in the aortic wall and periaortic structures. Areas of high signal intensity on spin echo images within the thrombus and aortic wall may indicate instability of the aneurysm (Sakamoto, 2010; Russo, 2006b). High signal is

emphasized by using fat suppressed T1-weighted sequences. Also, contrast enhanced MRA, using time resolved techniques, allows visualization of the Adamkiewicz artery (Bley, 2010), providing information that is important in planning the surgical repair of an aneurysm, thus avoiding postoperative neurologic deficit secondary to spinal cord ischemia (Nijenhuis, 2006; Yoshioka, 2006).

4.2 Acute aortic syndrome

Acute Aortic Syndrome includes dissection, intramural hematoma, and penetrating ulcer. In all three conditions, MRI may have a role with similar diagnostic capability or advantages over CT.

4.2.1 Aortic dissection

Aortic dissection is a life-threatening condition requiring prompt diagnosis and treatment. This condition occurs when blood dissects into the media of the aortic wall through an intimal tear. Classification of aortic dissections has been based traditionally on anatomic location and time from onset. The 14-day period after onset has been designated as the acute phase, because morbidity and mortality rates are highest (15%–25%), and surviving patients typically stabilize during this period. The Stanford classification distinguishes aortic dissection into type A or B, whether the ascending aorta is involved or spared, respectively. This classification is based fundamentally on prognostic factors: type A dissection necessitates urgent surgical repair, but most type B dissections can be managed conservatively. Hence, accurate recognition with imaging of anatomic details of the dissection is essential for successful management (Cigarroa, 1993). The diagnostic goals of imaging are a clear anatomic delineation of the intimal flap and its extension and the detection of the entry and re-entry sites and branch vessel involvement (Fig9).

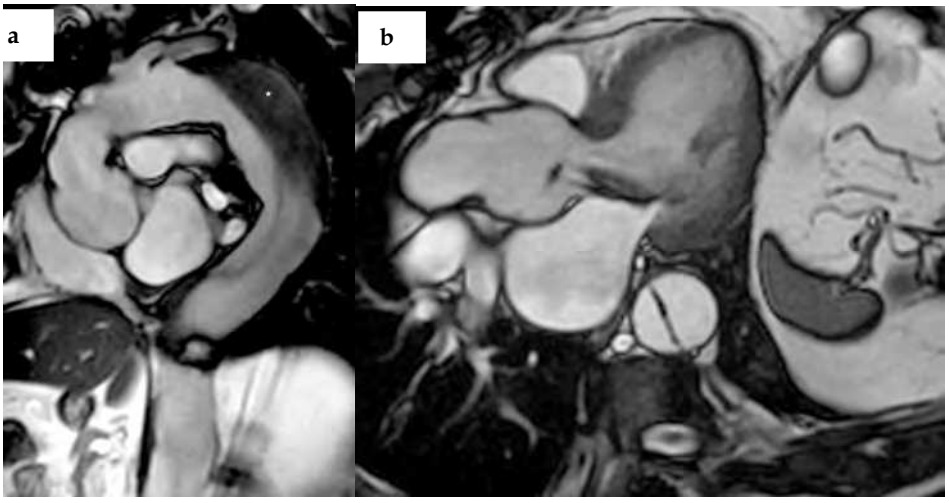

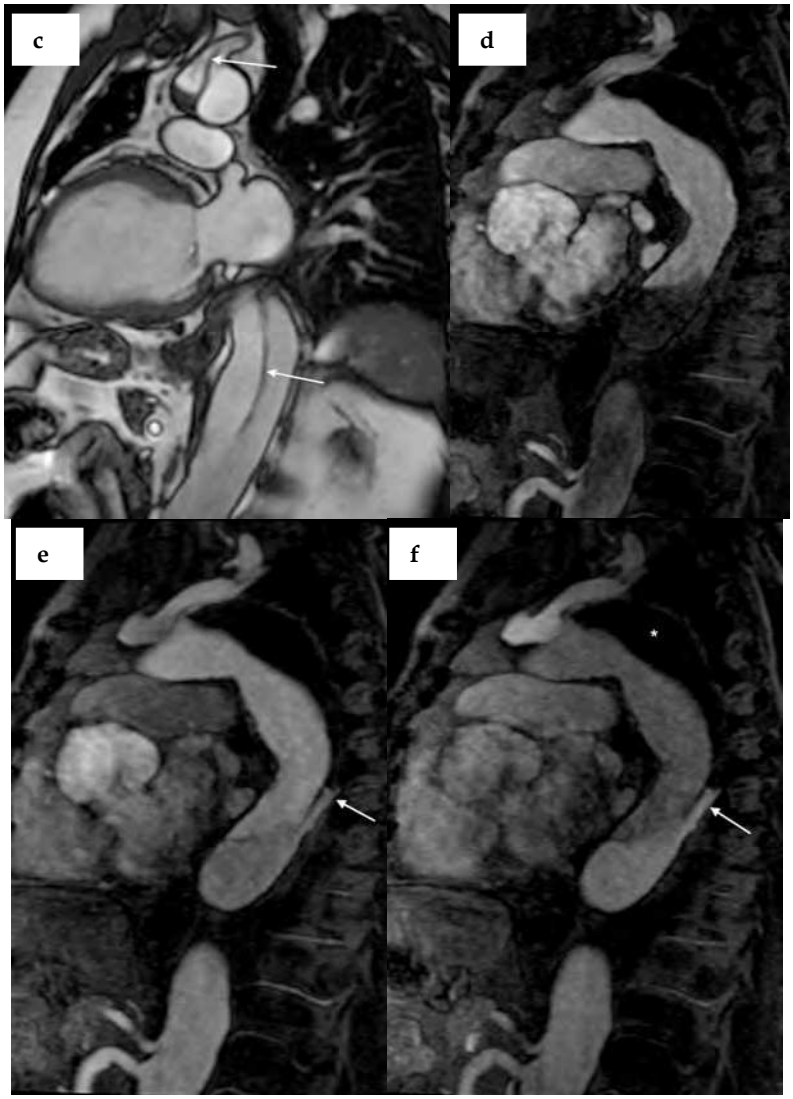

Aortic root dilatation with severe aortic insufficiency (50%) is noted (b) on axial heart three chambers view bSSFP images. This sentence belongs to figure 9 legend.

Fig. 9. ECG gated bSSFP (a, b, c) and 3D contrast-enhanced MR angiography of aortic dissection (d, e, f). Sequelae of prior surgical repair of the ascending aorta with stable type A aortic dissection with thrombosis of the false lumen (asterisk, a, f) at the level of the arch and with a persistent but unchanged dissection flap originating in the aortic arch near to the left subclavian takeoff. The arch vessels arise from the true lumen and the left subclavian artery is involved by dissection. The distal arch and thoracic aorta are dilated and retrograde fill of the false lumen is depicted on CE-MRA (d, e). The dissection flap extends throughout the thoracic and abdominal aorta and into the right common and external iliac arteries.

With current technology, MR imaging is the most accurate tool for detection of these features of the dissection (Prince, 1993; LaRoy, 1989; Roberts, 2001; Shiga, 2006). Occasionally MR can also demonstrate "aortic cobwebs", which are fibroelastic bands formed during the dissection process that project from the false lumen wall (Williams, 1994). Detection of these bands facilitates the distinction of the false from the true lumen, as they are located in the false lumen. On spin-echo images, flow in the true lumen is usually signal void, whereas flow in the false lumen can be signal void or high in signal intensity depending upon the velocity of blood flow. Slow flow in the false lumen of a dissection may be difficult to differentiate from thrombosis on spin-echo images (Fig5).
The role of conventional spin-echo imaging is limited because CE MRA/MRI imaging are all fast, accurate, and reproducible techniques for the demonstration of dissection. CE-MRA/MRI techniques reliably differentiate slow flow, which is high in signal intensity on these images, from thrombus, which is low to intermediate in signal intensity. Breath - hold CE-MRA images provide sharp detail and demonstrate the full extent of dissection, the entry site, the location of the intimal flap. The entry site, intimal flap, and branch vessel origins are better shown on individual sections than on 3D MIP reconstructions. The serial acquisition of two data sets provides dynamic flow information, which often demonstrates lack of opacification on early post contrast images followed by delayed enhancement of the false lumen, which is apparent in cases with slow flow. TR-MRA can also be used. Its temporal resolution allows a confident distinction between the true and false lumen (Fig3).

4.2.2 Penetrating aortic ulcers and intramural dissecting hematoma

Penetrating aortic ulcers result from ulcerated atherosclerotic plaques that penetrate the internal elastic lamina and may lead to hematoma formation within the media of the aortic wall, false aneurysm, and may progress to transmural rupture of the aorta.
Intramural hematoma (Fig10) usually results from spontaneous rupture of the aortic wall vasa vasorum, from a penetrating atherosclerotic ulcer. Extensive atherosclerotic changes are usually present in the aorta in the latter condition (Welch, 1990). The diagnostic MR imaging findings in penetrating atherosclerotic ulcer is a craterlike outpouching extending beyond the contour of the aortic lumen (Yucel, 1990; Hayashi, 2000; Macura, 2003). Mural thickening with high or intermediate signal intensity T1-weighted fat suppressed gradient- or on spin-echo sequences indicates the formation of intramural hematoma. Intramural hematoma most frequently involves the ascending or proximal descending aorta. The clinical presentation is similar to dissection: severe chest pain radiating to the back. Because of the similarity between the two entities, intramural hematoma is classified in the same way as aortic dissection: type A when the ascending aorta is involved and type B when involvement is limited to the descending aorta. (Litmanovich, 2009; Nienaber, 1995). The importance of intramural hematoma is that it can be a precursor of aortic dissection, representing either an early stage or a variant of dissection (Litmanovich, 2009; Nienaber, 1995; Cho, 2004). Complete resolution of the aortic hematoma is seen occasionally, but complications such as fluid extravasation with pericardial, pleural, and periaortic hematoma or aortic rupture may occur at the time of the onset or during the follow-up period. Progression of intramural hematoma to overt dissection and rupture has been reported in 32% of the cases, particularly when the ascending aorta is involved (Sakamoto, 2010).
Intramural hematoma can be identified as crescentic thickening of the aortic wall with abnormal signal intensity. Intramural hematoma is high in signal intensity on both T1 - and T2-weighted images and can be differentiated from chronic mural thrombus, which is low in

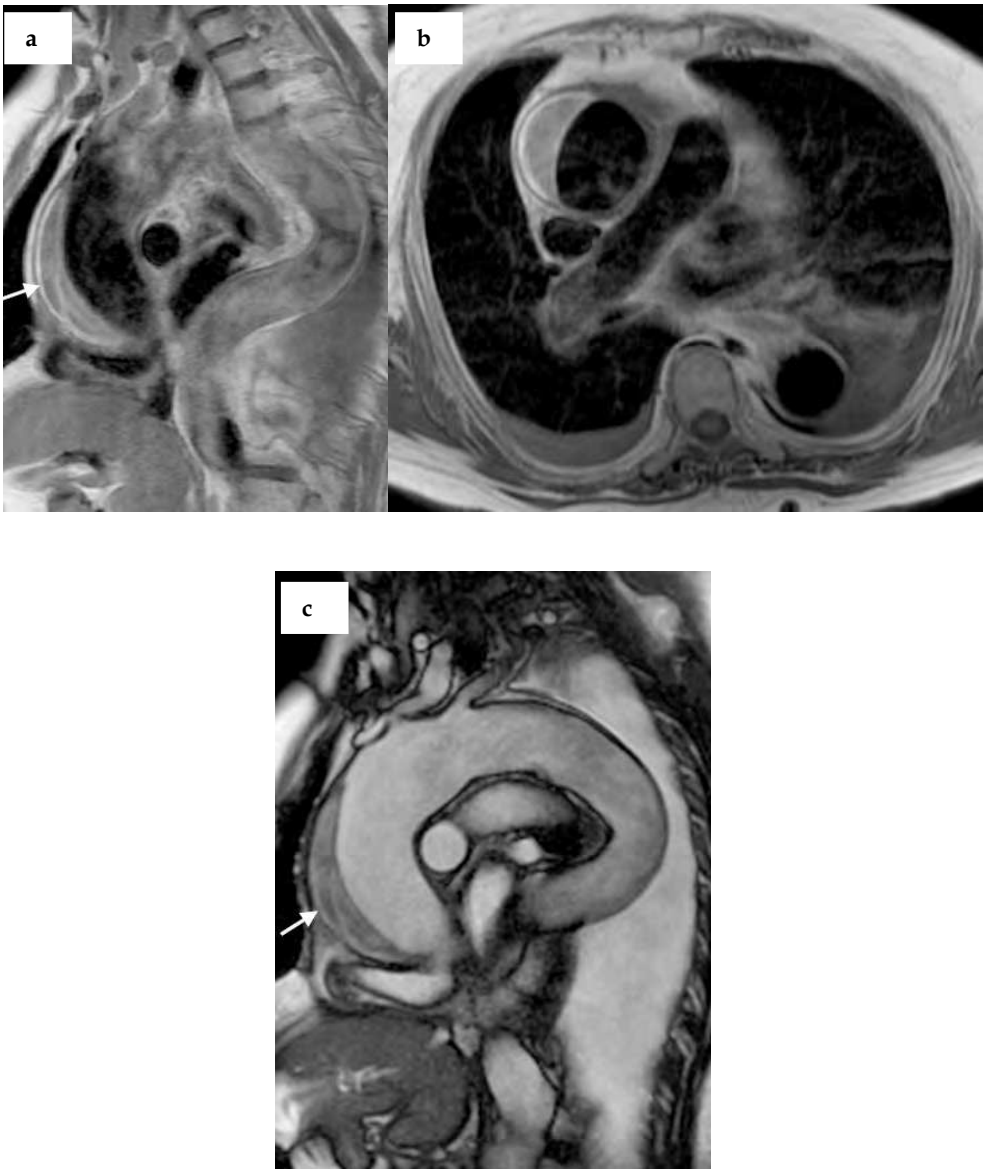

Fig. 10. Double inversion recovery spin echo MR imaging of intramural hematoma (a, b). On a T1-weighted spin echo MR image, intramural hematoma of the ascending thoracic aorta shows a crescentic local wall thickening with high signal intensity (arrow, a) caused by the presence of methemoglobin (subacute stage). Two-chamber view oblique sagittal bSSFP (c) shows in the same topography, a crescentic low signal intensity area.

signal intensity (Yucel, 1990). The combination of CE-MRA images to define the aortic lumen and 3D-GRE images to demonstrate the wall thickness in deep aortic ulcers may be the most effective means for evaluating this entity. Fat suppression images can be helpful in differentiating high-signal intramural hematoma from surrounding mediastinal fat. T1-weighted spin echo MR imaging (black blood techniques), can also be used to evaluate the aortic wall (Sakamoto, 2010; Litmanovich, 2009).

5. Future perspectives and challenges

There is growing concern among clinicians for the necessity of diagnostic, cost effective and safe imaging, with ionizing radiation being a major concern in some patients (Picano, 2007). At present, the routine use of MR angiography/MRI in the emergency setting for acute aortic syndrome is not established, reflecting lesser availability than CT and greater problems with motion artifacts compromising some studies. Nevertheless, there are increasing indications of MRI, such as young individuals, pregnant patients, and high-risk to iodinated contrast agent nephropathy. CE-MRA and 3D-GRE MRI with gadolinium have been shown to be a reliable and safe method for imaging the aorta. Motion artifacts remain the major cause for study compromise if patients are not able to comply with breathholding. Recent developments, such as 3D-GRE with a radial K-space acquisition (Azevedo, 2011), have been shown to provide adequate motion resistant imaging in the abdomen. This sequence may also provide diagnostic images in the chest, in combination with a blood contrast agent such as gadofosveset trisodium, probably allowing motion-resistant steady-state contrast enhanced MRA of the chest. Other techniques, such as non-contrast enhanced real-time SSFP can also provide rapid acquisition, motion resistant images in critically ill patients. Newer scanner with greater numbers of channels will also permit higher parallel imaging acquisition sequences with considerably shorter acquisition, in general important for patients who are critically ill.

6. Conclusion

In conclusion, MRI can provide a comprehensive evaluation of the aorta, using different and often complementary approaches, with protocols tailored individually to the clinical question, including morphological and functional evaluation. It is the authors' opinion that the recent development of MRI hardware and software facilitating faster imaging with the growing concern of safety, regarding ionizing radiation will further increase the importance of MRI in the study of vascular thoracic pathology, in the emergency department setting.

7. References

Altun E, Martin DR, Wertman R, et al. (2009a) Nephrogenic Systemic Fibrosis: Change in Incidence Following a Switch in Gadolinium Agents and Adoption of a Gadolinium Policy: Report from Two U.S. Universities. Radiology; 253(3):689-96 .

Altun E, Semelka RC, Cakit C. (2009b) Nephrogenic systemic fibrosis and management of high-risk patients. Acad Radiol; 16(7):897-905.b

Altun E, Elias Jr. J, Birchard KR, et al. (2010) Chest. In: Semelka RC, ed. Abdominal Pelvic MRI. 3rd edition. Wiley-Blackwell, New Jersey;

Amano Y, Takahama K, Kumita S. (2008) Non-contrast-enhanced MR angiography of the thoracic aorta using cardiac and navigator-gated magnetization-prepared three-dimensional steady-state free precession. J Magn Reson Imaging; 27(3):504-9.

Azevedo RM, De Campos RO, Ramalho M, et al. (2011) Free Breathing Three-Dimensional T1-Weighted Gradient-Echo Sequence Using Radial Data Sampling In Abdominal Imaging: Preliminary Observations. AJR Am. J. Roentgenol; 197: 10.2214/ AJR.10.5881

Bader TR, Semelka RC, Pedro MS, et al. (2002) Magnetic resonance imaging of pulmonary parenchymal disease using a modified breath-hold 3D gradient-echo technique: initial observations. J Magn Reson Imaging; 15:31–8.

Bhargavan M, Sunshine JH, Lewis RS, et al. (2010) Frequency of use of imaging tests in the diagnosis of pulmonary embolism: effects of physician specialty, patient characteristics, and region. AJR Am J Roentgenol; 194:1018-1026.

Bi X, Deshpande V, Simonetti O, et al. (2005) Threedimensional breathhold SSFP coronary MRA: a comparison between 1.5T and 3.0T. J Magn Reson Imaging; 22(2):206-12

Bickerstaff LK, Pairolero PC, Hollier LH, et al. (1982) Thoracic aortic aneurysms: a population-based study. Surgery; 92:1103–1108

Bley TA, Duffek CC, François CJ, et al. Presurgical localization of the artery of Adamkiewicz with time-resolved 3.0-T MR angiography.(2010) Radiology; 255(3):873-81.

Boiselle PM, White CS, eds. (2007) New techniques in cardiothoracic imaging. New York, NY: Informa HealthCare: 105–126

Bonser RS, Pagano D, Lewis ME, et al. (2000) Clinical and patho-anatomical factors affecting expansion of thoracic aortic aneurysms. Heart; 84:277–83.

Bradley WG Jr, Waluch V. (1985) Blood flow: magnetic resonance imaging. Radiology; 154(2):443–50.

Caravan P, Parigi G, Chasse JM, et al. (2007) Albumin binding, relaxivity, and water exchange kinetics of the diastereoisomers of MS-325, a gadolinium (III)-based magnetic resonance angiography contrast agent. Inorg Chem. 6; 46(16):6632-9.

Carr JC, Simonetti O, Bundy J, et al. (2001) Cine MR angiography of the heart with segmented true fast imaging with steady-state precession. Radiology; 219(3):828–34.

Cho KR, Stanson AW, Potter DD, et al. (2004) Penetrating atherosclerotic ulcer of the descending thoracic aorta and arch. J Thorac Cardiovasc Surg; 127:1393-1399.

Cigarroa JE, Isselbacher EM, DeSanctis RW, et al. (1993) Diagnostic imaging in the evaluation of suspected aortic dissection. Old standards and new directions. N Engl J Med;328:35–43.

Coady MA, Rizzo JA, Hammond GL, et al. (1997) What is the appropriate size criterion for resection of thoracic aortic aneurysms? J Thorac Cardiovasc Surg; 113:476–491.

Crawford ES, DeNatale RW. (1986) Thoraco-abdominal aortic aneurysm: observations regarding the natural course of the disease. J Vasc Surg; 3: 578–582

Czum JM, Corse WR, Ho VB. (2005) MR angiography of the thoracic aorta. Magn Reson Imaging Clin N Am ;13:41–64.

De Campos RO, Herédia V, Ramalho M, et al. (2011) Quarter-dose (0.025 mmol/kg) gadobenate dimeglumine for abdominal MRI in patients at risk for nephrogenic systemic fibrosis: preliminary observations. AJR Am J Roentgenol; 196(3):545-52

Debatin JF, Hany TF. (1998) MR-based assessment of vascular morphology and function. Eur Radiol; 8:528–39.

Earls JP, Ho VB, Foo TK, et al. (2002) Cardiac MRI: recent progress and continued challenges. J Magn Reson Imaging; 16:111–27.

Elefteriades JA. (2002) Natural history of thoracic aortic aneurysms: indications for surgery, and surgical versus nonsurgical risks. Ann Thorac Surg; 74:S1877–S1880; discussion S1892–S1898

Elefteriades JA, Tranquilli M, Darr U, et al. (2005) Symptoms plus family history trump size in thoracic aortic aneurysm. Ann Thorac Surg; 80:1098–1100

Fattori R, Nienaber CA. (1999) MRI of acute and chronic aortic pathology: pre-operative and postoperative evaluation. J Magn Reson Imaging;10:741–50.

Foo TK, Saranathan M, Prince MR, et al. (1997) Automated detection of bolus arrival and initiation of data acquisition in fast, three-dimensional, gadolinium enhanced MR angiography. Radiology; 203: 275–80.

Fuchs F, Laub G, Othomo K. (2003) TrueFISP-technical considerations and cardiovascular applications. Eur J Radiol; 46:28–32

Gebker R, Gomaa O, Schnackenburg B, et al. (2007) Comparison of different MRI techniques for the assessment of thoracic aortic pathology: 3D contrast enhanced MR angiography, turbo spin echo and balanced steady state free precession. Int J Cardiovasc Imaging; 23(6):747–56.

Geisinger MA , Risius B , O'Donnell J, et al. (1985) Thoracic aortic dissections: magnetic resonance imaging . Radiology; 155 (2): 407-412.

Griffin M, Grist TM, François CJ. (2009) Dynamic Four-Dimensional MR Angiography of the Chest and Abdomen. Magn Reson Imaging Clin N Am 17; 77–90.

Hany TF, Mckinnon GC, Leung DA, et al. (1997) Optimization of contrast timing for breath-holding threedimensional MR angiography. J Magn Reson Imaging; 7:551–6.

Hartmann M, Wiethoff AJ, Hentrich HR, et al. (2006) Initial imaging recommendations for Vasovist angiography. Eur Radiol; 16(Suppl 2):B15–B23

Hayashi H, Matsuoka Y, Sakamoto I, et al. (2000) Penetrating atherosclerotic ulcer of the aorta: imaging features and disease concept. Radiographics; 20:995-1005.

Jha S, Ho A, Bhargavan M, Owen JB, Sunshine JH. (2010) Imaging evaluation for suspected pulmonary embolism: what do emergency physicians and radiologists say? AJR Am J Roentgenol; 194:W38-48.

Karabulut N, Martin DR, Yang M, et al. (2002) MR Imaging of the chest using a contrast-enhanced breath-hold modified three-dimensional gradient-echo technique: comparison with two-dimensional gradient-echo and multidetector CT. AJR Am J Roentgenol; 179: 1225–33.

Klessen C, Hein PA, Huppertz A et al. (2007) First-pass whole-body magnetic resonance angiography (MRA) using the blood-pool contrast medium gadofosveset trisodium: comparison to gadopentetate dimeglumine. Invest Radiol; 42:659–664

Kluge A, Muller C, Hansel J, et al. (2004) Real-time MR with TrueFISP for the detection of acute pulmonary embolism: initial clinical experience. Eur Radiol; 14:709–18.

Korosec FR, Frayne R, Grist TM, Mistretta CA. (1996) Time-resolved contrast-enhanced 3D MR angiography. Magn Reson Imaging; 8:322–344

Krinsky G, Rofsky N, Flyer M, et al. (1996) Gadolinium enhanced three dimensional MR angiography of acquired arch vessels disease. Am J Roentgenol; 167:981–7.

Krinsky G, Rofsky N, De Corato DR, et al.(1997) Thoracic aorta: comparison of gadolinium-enhanced three dimensional MR angiography with conventional MR imaging. Radiology; 202:183–93.

Krinsky GA, Reuss PM, Lee VS, et al. (1999) Thoracic aorta: comparison of single-dose breath-hold and double-dose non-breath-hold gadolinium-enhanced three-dimensional MR angiography. AJR Am J Roentgenol; 173:145–150

Krishnam MS, Tomasian A, Deshpande VS, et al. (2008) Non-contrast 3D SSFP MR angiography of the whole chest using non-selective RF excitation over a large field of view: comparison with single-phase 3D contrast-enhanced MRA. Invest Radiol; 43(6):411–420

Krishnam MS, Tomasian A, Malik S, et al. (2010) Image quality and diagnostic accuracy of unenhanced SSFP MR angiography compared with conventional contrast-enhanced MR angiography for the assessment of thoracic aortic diseases. Eur Radiol; 20(6):1311-20.

Kunz RP, Oberholzer K, Kuroczynski W, et al. (2004) Assessment of chronic aortic dissection: contribution of different ECG-gated breath-hold MRI techniques. AJR Am J Roentgenol;182(5):1319–26.

LaRoy LL , Cormier PJ , Matalon TA et al. (1989) Imaging of abdominal aortic aneurysms . AJR Am J Roentgenol; 152 (4): 785-792.

Lauffer RB, Parmelee DJ, Dunham SU et al. (1998) MS-325: albumin-targeted contrast agent for MR angiography. Radiology; 207:529–538

Lee VS, Martin DJ, Krinsky GA et al. (2000) Gadolinium- enhanced MR angiography: Artifacts and pitfalls. AJR Am J Roentgenol; 175:197-205

Litmanovich D, Bankier AA, Cantin L, et al. (2009) CT and MRI in diseases of the aorta. AJR Am J Roentgenol; 193(4):928-40.

Lohan DG, Krishnam M, Saleh R, et al. (2008) MR Imaging of the Thoracic Aorta. Magn Reson Imaging Clin N Am; 16: 213–234

Lohan DG, Krishnam M, Saleh R, et al. (2008b) Time-Resolved MR Angiography of the Thorax. Magn Reson Imaging Clin N Am; 16: 235–248

Macura KJ, Szarf G, Fishman EK, et al. (2003) Role of computed tomography and magnetic resonance imaging in assessment of acute aortic syndromes. Semin Ultrasound CT MR; 24:232-54.

Marks B, Mitchell DG, Simelaro JP. (1997) Breathholding in healthy and pulmonary-compromised populations: Effects of hyperventilation and oxygen inspiration. J Magn Reson Imaging; 7:595-597

Martin DR, Semelka RC, Chapman A, et al. (2009) Nephrogenic systemic fibrosis versus contrast-induced nephropathy: risks and benefits of contrast-enhanced MR and CT in renally impaired patients. J Magn Reson Imaging; 30(6):1350-6.

Matsunaga N, Hayashi K, Okada M, et al. (2009) Magnetic resonance imaging features of aortic diseases. Top Magn Reson Imaging; 14(3):253–66.

McCauley TR, Monib A, Dickey KW, et al. (1994) Peripheral vascular occlusive disease: accuracy and reliability of time-of-flight MR angiography. Radiology; 192:351–7.

Neimatallah MA, Ho VB, Dong Q, et al. (1999) Gadolinium based 3D magnetic resonance angiography of the thoracic vessels. J Magn Reson Imaging; 10: 758–70.

Nienaber CA, von Kodolitsch Y, Petersen B, et al. (1995) Intramural hemorrhage of the thoracic aorta: diagnosis and therapeutic implications. Circulation; 92:1465-72.

Nijenhuis RJ, Jacobs MJ, van Engelshoven JM, et al. (2006) MR angiography of the Adamkiewicz artery and anterior radiculomedullary vein: postmortem validation. AJNR Am J Neuroradiol; 27:1573–5.

Nissen JC, Attenberger UI, Fink C, et al. (2009) Thoracic and abdominal MRA with gadofosveset: influence of injection rate on vessel signal and image quality. Eur Radiol; 19(8):1932-8.

Pereles FS, McCarthy RM, Baskaran V, et al. (2002) Thoracic aortic dissection and aneurysm: evaluation with nonenhanced true FISP MR angiography in less than 4 minutes. Radiology; 223:270–4.

Picano E, Vano E, Semelka R, Regulla D. (2007) The American College of Radiology white paper on radiation dose in medicine:deep impact on the practice of cardiovascular imaging. Cardiovasc Ultrasound; 5:37.

Potthast S, Mitsumori L, Stanescu LA, et al. (2010) Measuring aortic diameter with different MR techniques: comparison of three-dimensional (3D) navigated steady-state free-precession (SSFP), 3D contrast-enhanced magnetic resonance angiography (CE-MRA), 2D T2 black blood, and 2D cine SSFP J Magn Reson Imaging; 31(1):177-84.

Prince MR, Yucel EK, Kaufman JA, et al. (1993) Dynamic gadolinium- enhanced three-dimensional abdominal MR arteriography. J Magn Reson Imaging; 3:877–81.

Prince MR, Narasimham DL, Jacoby WT, et al. (1996) Three dimensional gadolinium-enhanced MR angiography of the thoracic aorta. AJR Am J Roentgenol; 166: 1387–97.

Riederer SJ, Bernstein MA, Breen JF, et al. (2000) Three dimensional contrast-enhanced MR angiography with real-time fluoroscopic triggering: design specifications and technical reliability in 330 patient studies. Radiology; 215:584–93.

Roberts DA. (2001) Magnetic resonance imaging of thoracic aortic aneurysm and dissection . Semin Roentgenol; 36 (4): 295-308 .

Rohrer M. (2005) Comparison of magnetic properties of MRI contrast media solutions at different magnetic field strengths. Invest Radiol; 40:715–724

Russo V, Renzulli M, Palombara CL, et al. (2006) Congenital diseases of the thoracic aorta: role of MRI and MRA. Eur Radiol; 16:676–84.

Russo V, Renzulli M, Buttazzi K, et al. (2006b) Acquired diseases of the thoracic aorta: role of MRI and MRA. Eur Radiol; 16:852–65.

Sakamoto I, Sueyoshi E, Uetani M. (2010) MR Imaging of the Aorta. Magn Reson Imaging Clin N Am; 18: 43–55

Schneider G, Prince MR, Meaney JM et al. (2005) Magnetic Resonance Angiography: Techniques, Indications, and Practical Applications. Milan, Italy: Springer.

Schoenberg SO, Wunsch C, Knopp MV, et al. (1999) Abdominal aortic aneurysm. Detection of multilevel vascular pathology by time-resolved multiphase 3D gadolinium MR angiography: initial report. Invest Radiol; 34(10):648-59

Shiga T, Wajima Z, Apfel CC, Inoue T, Ohe Y. (2006) Diagnostic accuracy of transesophageal echocardiography, helical computed tomography, and magnetic resonance imaging for suspected thoracic aortic dissection: systematic review and meta-analysis. Arch Intern Med; 166:1350–1356

Sodickson DK, McKenzie CA, Li W, et al. (2000) Contrast enhanced 3D MR angiography with simultaneous acquisition of spatial harmonics: a pilot study. Radiology; 217(1):284–9.

Stehling MK, Holzknecht NG, Laub G, et al. (1996) Singleshot T1- and T2-weighted magnetic resonance imaging of the heart with black blood: preliminary experience. MAGMA; 4(3–4):231–40.

Tatli S, Yucel EK, Lipton MJ. (2004) CT and MR imaging of the thoracic aorta: current techniques and clinical applications. Radiol Clin North Am; 42:565–585, vi

Tomasian A, Lohan DG, Laub G, et al. (2008) Noncontrast 3D steady state free precession magnetic resonance angiography of the thoracic central veins using nonselective radiofrequency excitation over a large field of view: initial experience. Invest Radiol; 43(5):306–313

Welch TJ, Stanson AW , Sheedy PF 2nd et al. (1990) Radiologic evaluation of penetrating aortic atherosclerotic ulcer . Radiographics; 10 (4): 675-685.

Wertman R, Altun E, Martin DR, et al. (2008) Risk of nephrogenic systemic fibrosis: evaluation of gadolinium chelate contrast agents by four American universities. Radiology; 248:799–806.

Williams DM, Joshi A, Dake MD et al. (1994) Aortic cobwebs: an anatomic marker identifying the false lumen in aortic dissection imaging and pathologic correlation . Radiology; 190 (1): 167-174.

Winterer JT, Lehnhardt S, Schneider B, et al. (1999) MRI of heart morphology. Comparison of nongradient echo sequences with single and multislice acquisition. Invest Radiol; 34(8):516–22.

Yoshioka K, Niinuma H, Ehara S, et al. (2006) MR angiography and CT angiography of the artery of Adamkiewicz: state of the art. Radiographics; 26:S63–73.

Yu T, Zhu X, Tang L, et al. (2007) Review of CT angiography of aorta. Radiol Clin North Am; 45:461–483, viii

Yucel EK , Steinberg FL , Egglin TK et al. (1990) Penetrating aortic ulcers: diagnosis with MR imaging . Radiology;177(3):779-788.

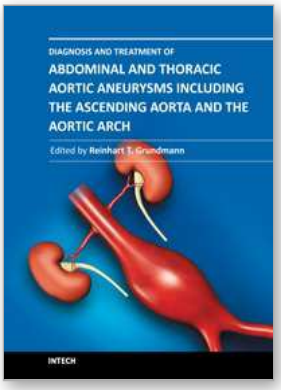

Diagnosis and Treatment of Abdominal and Thoracic Aortic Aneurysms Including the Ascending Aorta and the Aortic Arch
Edited by Prof. Reinhart Grundmann

ISBN 978-953-307-524-2
Hard cover, 208 pages
Publisher InTech
Published online 22, June, 2011
Published in print edition June, 2011

This book considers diagnosis and treatment of abdominal and thoracic aortic aneurysms. It addresses vascular and cardiothoracic surgeons and interventional radiologists, but also anyone engaged in vascular medicine. The book focuses amongst other things on operations in the ascending aorta and the aortic arch. Surgical procedures in this area have received increasing attention in the last few years and have been subjected to several modifications. Especially the development of interventional radiological endovascular techniques that reduce the invasive nature of surgery as well as complication rates led to rapid advancements. Thoracoabdominal aortic aneurysm (TAAA) repair still remains a challenging operation since it necessitates extended exposure of the aorta and reimplantation of the vital aortic branches. Among possible postoperative complications, spinal cord injury (SCI) seems one of the most formidable morbidities. Strategies for TAAA repair and the best and most reasonable approach to prevent SCI after TAAA repair are presented.

How to reference
In order to correctly reference this scholarly work, feel free to copy and paste the following:

Vasco Herédia, Miguel Ramalho, Sérgio Duarte, Rafael O.P. de Campos, Mateus Hernandez, Nuno Jalles Tavares and Richard C. Semelka (2011). Magnetic Resonance Imaging of the Thoracic Aorta: A Review of Technical and Clinical Aspects, Including Its Use in the Evaluation of Aneurysms and Acute Vascular Conditions, Diagnosis and Treatment of Abdominal and Thoracic Aortic Aneurysms Including the Ascending Aorta and the Aortic Arch, Prof. Reinhart Grundmann (Ed.), ISBN: 978-953-307-524-2, InTech, Available from: http://www.intechopen.com/books/diagnosis-and-treatment-of-abdominal-and-thoracic-aortic-aneurysms-including-the-ascending-aorta-and-the-aortic-arch/magnetic-resonance-imaging-of-the-thoracic-aorta-a-review-of-technical-and-clinical-aspects-includin

INTECH
open science | open minds

InTech Europe
University Campus STeP Ri
Slavka Krautzeka 83/A
51000 Rijeka, Croatia
Phone: +385 (51) 770 447
Fax: +385 (51) 686 166
www.intechopen.com

InTech China
Unit 405, Office Block, Hotel Equatorial Shanghai
No.65, Yan An Road (West), Shanghai, 200040, China
中国上海市延安西路65号上海国际贵都大饭店办公楼405单元
Phone: +86-21-62489820
Fax: +86-21-62489821